

This document downloaded from
vulcanhammer.net vulcanhammer.info
Chet Aero Marine



Don't forget to visit our companion site
<http://www.vulcanhammer.org>

Use subject to the terms and conditions of the respective websites.

Concrete Pile Head Response to Impact

Don C. Warrington, PhD., P.E.
University of Tennessee at Chattanooga
Department of Mechanical Engineering

The application of semi-infinite pile theory to the behaviour of driven piles has been studied since Parola (1970). Most of the effort, however, has been concentrated on piles which do not require a cushion between the pile head and the pile driving accessory, such as steel piles. Concrete piles, on the other hand, are generally driven with this additional cushion. In this paper the same type of semi-infinite type of analysis is applied to this problem. Both the case of a rigid pile head and a pile head which responds without reflection from the pile are studied using both closed-form and numerical solutions. Two case histories are included which illustrate the application of the method, along with parametric studies of both pile head conditions.

Keywords: concrete piles, hammer cushion, pile cushion, impact pile driving, semi-infinite piles

Introduction

Pile head response from impact of pile hammers using semi-infinite pile theory has been used since Parola (1970), and the theory is explained in Warrington (1997). Up until this time its use has primarily been with long steel piles, such as are used in offshore platforms and wind farms (Deeks and Randolph (1993); Warrington (1987, 2020).) Although some of these models include the use of hammers without a hammer cushion, none of them include a cushion between the driving accessory and the pile head. Most concrete piles are driven with such a cushion in order to reduce the compressive stresses during impact and, by extension, the tensile stresses that are reflected from the pile toe, especially during the early stages of driving when pile toe resistance is minimal.

Although semi-infinite pile solutions are most applicable to long offshore piles, they also reflect the initial response of shorter piles as well; this initial response is important in pile dynamics. In any case concrete piles have become longer and so this objection is not as relevant as it was in the past.

Up until now the only solution for this problem with concrete piles is that of Take, Valsangkar, and Randolph (1999). This solution is very elegant but suffers from the same complexities and limitations of other closed form solutions such as Deeks and Randolph (1993). The solution presented here is an extension of that of Warrington (2020), and utilises the same basic structure, which is as follows:

- Use of a dimensionless representation of the equations of motion, which was originally used by Parola (1970) and

developed further by Warrington (1987);

- Solution of the equations using Newmark's Method, which due to the simplicity of the system avoids the use of an explicit predictor-corrector structure; and
- Inclusion of the inextensibility of cushions by changing the stiffness matrix when the conditions warrant it.

Governing Equations and Basic Configuration

The basic configuration for hammers with a hammer cushion, concrete driving accessory (which will be referred to in this paper as a "cap") and a pile cushion is shown in Figure 1.

As mentioned above, the governing equations for this problem are reduced as shown in Warrington (2020) as follows:

$$\tau = t\omega_0 \quad (1)$$

where

$$\omega_0 = \sqrt{\frac{k_1}{m_1}} \quad (2)$$

Also,

$$z' = \frac{Z_3}{Z_1} \quad (3)$$

$$Z_3 = \sqrt{\rho EA_3} \quad (4)$$

$$Z_1 = \sqrt{m_1 k_1} \quad (5)$$

and

$$m' = \frac{m_1}{m_2} \quad (6)$$

My special thanks go to my department head, Dr. James C. Newman III, for his support of my research.

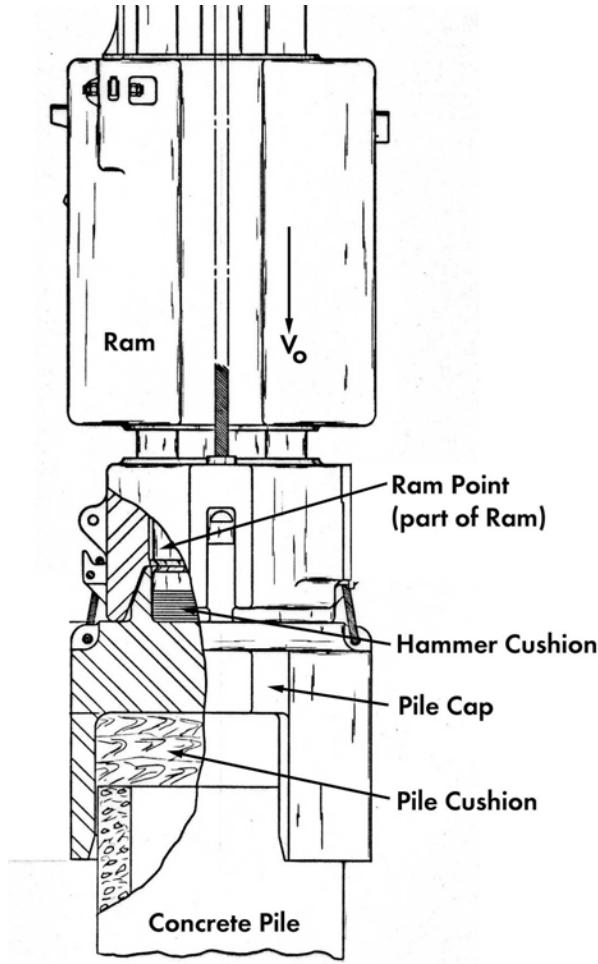


Figure 1. Hammer, Cushion, Cap and Pile Configuration for Concrete Piles

The following ratio is added:

$$k' = \frac{k_2}{k_1} \quad (7)$$

All this being the case, the reduced governing differential equations for the ram, cap and pile head respectively are

$$\frac{d^2}{d\tau^2} X_1(\tau) - X_2(\tau) + X_1(\tau) = 0 \quad (8)$$

$$\frac{d^2}{d\tau^2} X_2(\tau) + X_2(\tau) - X_1(\tau) + k' (X_2(\tau) - X_3(\tau)) = 0 \quad (9)$$

$$z' \frac{d}{d\tau} X_3(\tau) + k' (X_3(\tau) - X_2(\tau)) = 0 \quad (10)$$

This yields mass, damping and stiffness matrices as follows:

$$M = \begin{bmatrix} 1 & 0 & 0 \\ 0 & m'^{-1} & 0 \\ 0 & 0 & 0 \end{bmatrix} \quad (11)$$

$$C = \begin{bmatrix} 0 & 0 & 0 \\ 0 & 0 & 0 \\ 0 & 0 & z' \end{bmatrix} \quad (12)$$

$$K = \begin{bmatrix} 1 & -1 & 0 \\ -1 & 1 + k' & -k' \\ 0 & -k' & k' \end{bmatrix} \quad (13)$$

As before, the initial condition vector d_0 is null. The initial velocity vector is

$$v_0 = \begin{bmatrix} L_{sys} \\ 0 \\ 0 \end{bmatrix} \quad (14)$$

where

$$L_{sys} = \frac{V_0}{\omega_0} \quad (15)$$

For the case of a rigid pile head, Equation 8 is the same and Equations 9 and 10 are replaced by

$$\frac{d^2 X_2(\tau)}{d(\tau)^2} + X_2(\tau) - X_1(\tau) + k' X_2(\tau) = 0 \quad (16)$$

The mass and stiffness matrices for this set of equations (the damping matrix is null since there is no pile head) are as follows:

$$M = \begin{bmatrix} 1 & 0 \\ 0 & m'^{-1} \end{bmatrix} \quad (17)$$

$$K = \begin{bmatrix} 1 & -1 \\ -1 & 1 + k' \end{bmatrix} \quad (18)$$

Again the d_0 vector is null and the initial velocity vector is

$$v_0 = \begin{bmatrix} L_{sys} \\ 0 \end{bmatrix} \quad (19)$$

As was the case in Warrington (2020), Newmark's Method can be applied to both of these in the same way.

Closed Form Solution of Rigid Pile Model

Both Deeks and Randolph (1993) and Take et al. (1999) used closed-form solutions. The complexities of cushion and interface inextensibility make these solutions rather complex in practical use. The solution of a ram and cushion with a rigid cushion base is trivial but important for the understanding of these phenomena, as shown by Warrington (2020). For this problem the rigid base solution is equally important but not trivial.

The problem, at its simplest, is a two-degree of freedom system. The solution is presented extensively (den Hertog (1985); Kreyszig (1988); Meirovitch (2001); Thompson (1965).) With these systems there are variations. The most important variation from the system under consideration is a spring from the ram to a fixed point, which is lacking with pile systems. These solutions also feature simplifications such as the two masses being the same, the two spring constants being the same, or both. None of these conditions is guaranteed for the case at hand and significant differences can be expected.

Probably the solution that comes closest to replicating the system under consideration is that of Timoshenko and Young (1955). Considering this brings up another problem: this and the other solutions frequently require convenient assumptions to achieve a solution. For all their shortcomings, Deeks and Randolph (1993) and Take et al. (1999)'s use of Laplace transforms is probably the best way to solve these problems in closed form, in no small measure because the handling of the initial conditions is the most straightforward.

With this in mind, if the Laplace transforms of Equations 8 and 16 are taken and the initial conditions described above are applied, the following result is obtained:

$$s^2 \mathcal{L}(X_1(\tau), \tau, s) - L_{sys} - \mathcal{L}(X_2(\tau), \tau, s) + \mathcal{L}(X_1(\tau), \tau, s) = 0 \quad (20)$$

$$\frac{s^2 \mathcal{L}(X_2(\tau), \tau, s)}{m'} + \mathcal{L}(X_2(\tau), \tau, s) - \mathcal{L}(X_1(\tau), \tau, s) + k' \mathcal{L}(X_2(\tau), \tau, s) = 0 \quad (21)$$

Rearranging these equations and putting them into matrix form yields

$$\begin{bmatrix} s^2 + 1 & -1 \\ -1 & \frac{s^2}{m'} + 1 + k' \end{bmatrix} \begin{bmatrix} \mathcal{L}(X_1(\tau), \tau, s) \\ \mathcal{L}(X_2(\tau), \tau, s) \end{bmatrix} = \begin{bmatrix} L_{sys} \\ 0 \end{bmatrix} \quad (22)$$

Solving for the Laplace transforms,

$$\mathcal{L}(X_1(\tau), \tau, s) = \frac{(s^2 + m' + k' m') L_{sys}}{(s^2 + p_1^2)(s^2 + p_2^2)} \quad (23)$$

$$\mathcal{L}(X_2(\tau), \tau, s) = \frac{m' L_{sys}}{(s^2 + p_1^2)(s^2 + p_2^2)} \quad (24)$$

where

$$p_1 = 1/2 \sqrt{2 - 2\sqrt{m'^2 + 2k' m'^2 + 2m' + k'^2 m'^2} - 2k' m' + 1 + 2m' + 2k' m'} \quad (25)$$

$$p_2 = 1/2 \sqrt{2 + 2\sqrt{m'^2 + 2k' m'^2 + 2m' + k'^2 m'^2} - 2k' m' + 1 + 2m' + 2k' m'} \quad (26)$$

The inverse transforms (Starkey (1954)) and the solutions are as follows:

$$X_1(\tau) = \frac{L_{sys} (\sin(p_1 \tau) p_2 (p_1^2 - m' - k' m') + \sin(p_2 \tau) p_1 (m' + k' m' - p_2^2))}{p_1 p_2 (p_1^2 - p_2^2)} \quad (27)$$

$$X_2(\tau) = \frac{m' L_{sys} (\sin(p_2 \tau) p_1 - \sin(p_1 \tau) p_2)}{p_1 p_2 (p_1^2 - p_2^2)} \quad (28)$$

There are two things to note about these solutions.

First, both of the displacements—and by extension their derivatives—are linearly proportional to L_{sys} . This could be seen in the results by Warrington (2020) but is explicit here. (It is also worth noting that, for both the closed form and numerical solutions in this and the previous treatment, L_{sys} is input as a negative number in order to replicate the “downward positive” sign convention common in geotechnical engineering.)

Second, the values p_1 and p_2 are conventionally characterised as the two frequencies at which the system vibrates. In this case, however, they are not frequencies per se but ratios between each of the two vibrating frequencies and the natural frequency of the hammer/hammer cushion system, thus:

$$p_1 = \frac{\omega_1}{\omega_0} \quad (29)$$

and

$$p_2 = \frac{\omega_2}{\omega_0} \quad (30)$$

The ratio between these two frequencies should also be defined as

$$p_{rat} = \frac{p_2}{p_1} = \frac{\omega_2}{\omega_1} \quad (31)$$

Obviously this solution does not include either effects due to the pile itself or inextensibilities of the hammer or pile cushion. It can be used to verify the numerical methodology being used; however, in order to do that it is necessary to develop some kind of range of values to be used, which is the next subject to be considered.

Parameters for Parametric and Case Studies

Parametric Studies

Inspection of Equations 8, 9 and 10 shows that there are only three independent parameters: m' , z' and k' . If Equations 8 and 16 are considered, only z' is eliminated. Thus it

is important to determine a range of values for parameteric studies for either set of equations.

In Warrington (2020) the parameter ranges were based on Warrington (1987), namely $0.1 \leq z' \leq 1.6$ and $1 \leq m' \leq 10$. For the concrete piles it is reasonable to assume that one or both of these ranges will be different, and additionally k' will have to be considered. Pile driving equipment comes in a wide variety of configurations and, when modifications are made from factory specifications, the result is that the variations in equipment configurations is immense. For the purpose of this study the range of Vulcan pile driving equipment is considered. This product line has been developed over the course of more than a century and has been configured for a wide range of concrete piles. For this study hammers from the #1 hammer (15,000 ft-lbs) to the 560 (312,500 ft-lbs) are considered, and piles from 12" concrete to 54" cylinder piles are included. Hammer cushions employ the capblock follower configuration with micarta and aluminium cushion material, and piles include plywood in thicknesses of 6", 12" and 18". Cushion properties are per Goble and Rausche (1986) and many of the hammer, cushion and cap properties can be found in the same source.

The survey yielded the following results:

1. The mass ratio m' range that was used in Warrington (2020) can be used here as well. It is worth noting that these values tend to decrease with hammer size.

2. The impedance ratio z' range is much broader than that for steel piles, and should be set at $0.5 \leq z' \leq 3.5$. This obviously does not apply to the rigid pile head case.

3. The cushion stiffness ratio k' was the most difficult to quantify. In the end, although there are cases where hammer-pile combinations resulted in values outside of the range, for the purposes of this study $0.1 \leq k' \leq 1.0$.

It should be noted that, if other hammer configurations are considered, these ranges may vary significantly. The hammer cushions under consideration are potentially softer than others because their area is relatively small and the stack height relatively large since the capblock follower (which is an adaptation of the capblock shield concept developed by Raymond) was used following current factory preference. This would tend to lower values of k' . Heerema (1980) noted this about Vulcan hammers, albeit with a different cushion material (softer) and stack height (lower,) which to some extent compensate for each other. The use of stiffer cushions would also tend to increase values of z' as well.

Case Studies

There are two case studies that will be used in one or both of the models. The first is a Vulcan 06 hammer driving 12" solid square concrete piles; the second is a Vulcan 530 driving 36" solid square concrete piles. The parameters for each case are described in Table 1. For each hammer the results are analysed for both 6" and 18" thick pile cushions.

Table 1
Initial Parameters for Case Histories

Parameter	Vulcan 06	Vulcan 530
Rated Striking Energy, ft-lbs	19,500	150,000
Ram Weight, lbs	6,500	30,000
Efficiency, percent	67%	67%
Cushion stiffness, kips/ft	22,566	66,798
Hammer Impedance, lb-sec/ft	67,521	249,570
Ram Frequency, rad/sec	334.2	267.7
System Length, ft.	0.034	0.055
Initial driving accessory weight, lbs	1,030	6,200
Initial m'	5.58	4.13
Pile Cross-Sectional Area, in^2	144	1,296
Pile impedance, lb-sec/ft	57,938	521,438

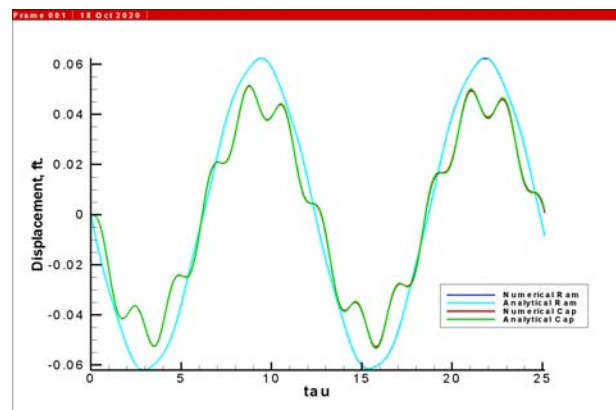


Figure 2. Analytical and Numerical Solutions, Rigid Pile, Vulcan 06 with 6" Cushion

For the Vulcan 530 case history, the driving accessory weight will be altered during the analysis.

Rigid Pile Model

The case study will be considered before the parameteric study in order to better illustrate the variables involved. Cushion inextensibility will be ignored; this will be sufficient to demonstrate the correspondence between the analytical solution and the numerical one, where only the primary variable (displacement) is considered. Peak values are thus consistent within the system cycle, making the parameteric study meaningful.

Case Study

For the rigid pile model only the Vulcan 06 case will be considered with two cushion thicknesses: 6" and 18". The graphical results for each of these cases are shown in Figures 2 and 3.

In both cases it was necessary to decrease the time step and, by doing so, reduce the numerical damping in order

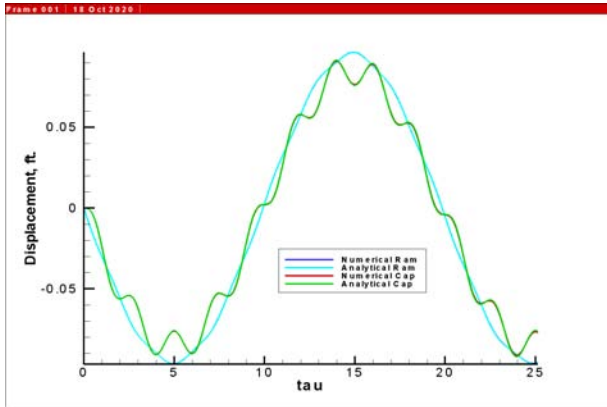


Figure 3. Analytical and Numerical Solutions, Rigid Pile, Vulcan 06 with 18'' Cushion

to achieve the correspondence of the two solutions shown, especially with the cap displacements. The fact that both solutions use the same time frame makes it easy to see that the lengthening/softening of the pile cushion decreases the frequencies of the system. The frequency ratio values will be shown in Table 3. The higher frequency affects the motion of the cap more than the ram.

Parametric Study

Although the rigid pile case needs to be used with care, there are some things that can be learned from it, especially since there are only two parameters that vary (m' and k'), as opposed to the three in the case with a yielding pile head. Some of the results are shown below.

Figures 4, 5 and 6 show the variation in p_1 , p_2 , and p_{rat} respectively. The results show that, in general, p_1 varies more with k' , p_2 with m' , and p_{rat} with both. The last parameter has its highest values with light caps (high m') and softer pile cushions (low k') and lowest values with heavy caps (low m') and stiffer pile cushions (high k'). In this case, there are no real values of m' and k' which allow for a $p_{rat} = 1$, thus the two-frequency regime is inherent in this system, as opposed to the single frequency one (obviously modified by the movement of the pile head) in Warrington (2020).

Figures 7 and 8 show the accelerations of the ram and cap respectively. In general the ram acceleration increases with the stiffer pile cushion, reflecting the reduced yield of the pile cushion in the system. This increase is not uniform and is not as pronounced for very heavy caps. The cap acceleration is fairly uniform until about $k' = 0.3$, below which it increases significantly. Very low pile cushion stiffnesses tend to increase the acceleration of the cap, something not generally considered when increasing the height of the pile cushion to effect lower stresses in the pile.

Figures 9 and 10 show the variations in maximum ram and cap displacement. This is a peak displacement and repeats it-

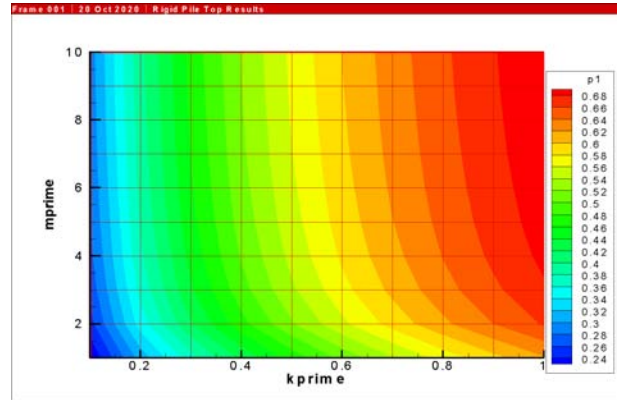


Figure 4. Parametric Study, Rigid Pile, Low Frequency Ratio

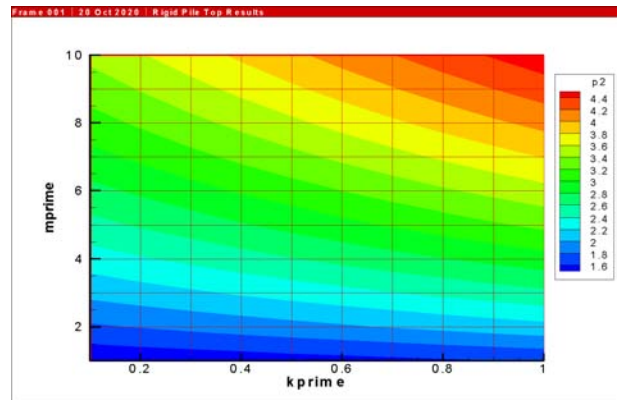


Figure 5. Parametric Study, Rigid Pile, High Frequency Ratio

self in the absence of inextensibility, as is evident in Figures 2 and 3. As was the case with cap acceleration, the peak ram displacement increases more rapidly with lower values of k' , as is the case with peak cap displacement.

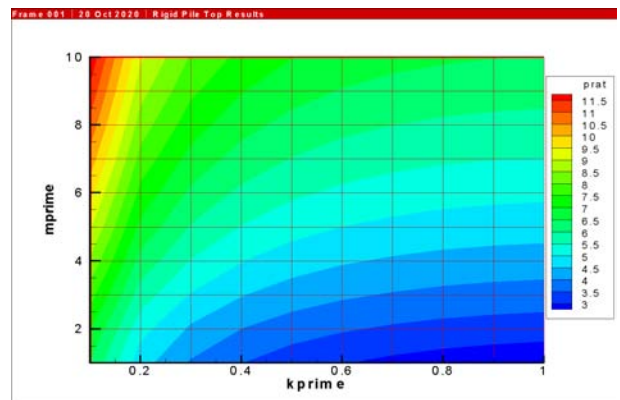


Figure 6. Parametric Study, Rigid Pile, Frequency Ratio Quotient

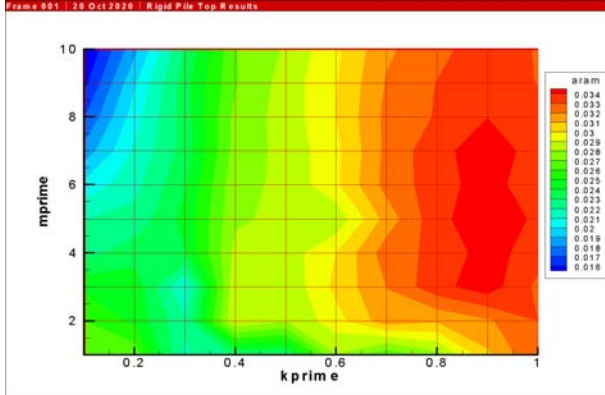


Figure 7. Parametric Study, Rigid Pile, Ram Acceleration

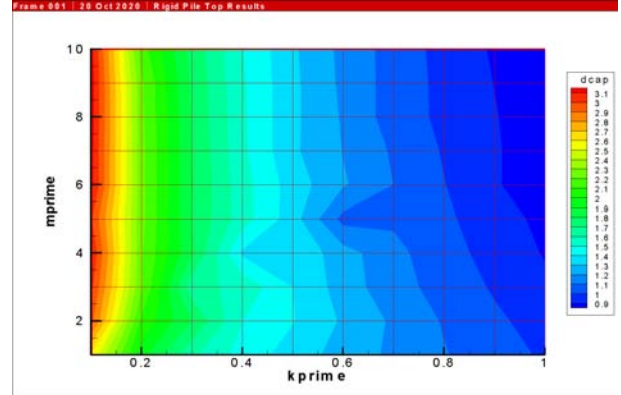


Figure 10. Parametric Study, Rigid Pile, Maximum Cap Displacement

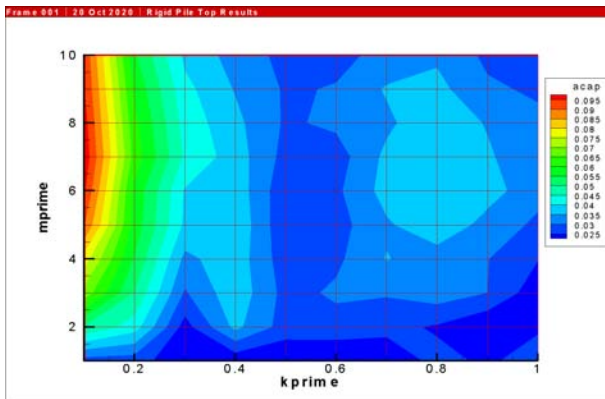


Figure 8. Parametric Study, Rigid Pile, Cap Acceleration

Semi-Infinite Pile Head Model

Parametric Study

In adding the effects of a yielding/semi-infinite model pile head, considerable complexity is added to the analysis. In this application, parametric studies in general can only dis-

cern the broadest trends. Applying this model to an actual jobsite requires recognition of the geotechnical requirements of the pile itself, which includes the size, type, length and other parameters. Matching a hammer to the pile, especially with larger piles, requires knowledge first of available equipment and how it is best used to install the pile under consideration.

The ranges of the parametric study for the three ratios m' , k' and z' were defined earlier. The variables under consideration are the same as those in Warrington (2020) except for the addition of the maximum pile head displacement, which in this case is different than that of the cap. For the entire parametric study $L_{sys} = 1$, which makes the results essentially dimensionless.

The most important thing to be determined in a parametric study is the variation of the dependent parameters subject to the independent ones. For this study a linear regression approach was employed, attempting to determine the variation according to the following equation:

$$y = m_{m'}m + m_{k'}k + m_{z'}z + b \quad (32)$$

This results in a non-dimensional “plane.” It is not evident that the slopes are constant; however, this approach can show the relative importance of each parameter by comparing the slopes for that parameter with each other. The routine was constructed including hammer and pile cushion inextensibilities; there are four states that the model can simulate during analysis, effected by changing the matrix of Equation 13:

- All cushions are in compression; the model operates with a full matrix.
- The pile cushion only goes into tension; Equation 13 becomes

$$K = \begin{bmatrix} 1 & -1 & 0 \\ -1 & 1 & 0 \\ 0 & 0 & 0 \end{bmatrix} \quad (33)$$

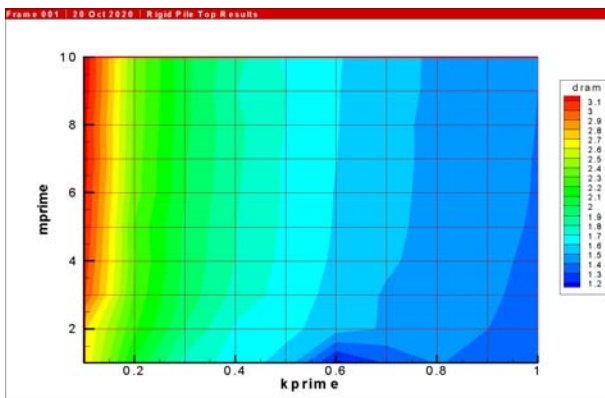


Figure 9. Parametric Study, Rigid Pile, Maximum Ram Displacement

Table 2
Parameter Slopes, y-intercepts and Coefficients of Determination for Parametric Study

y	$m_{k'}$	$m_{m'}$	$m_{z'}$	b	R^2
a_{ram}	-0.02	-0.01	0.05	0.57	0.62
a_{cap}	-0.54	0.20	0.06	0.89	0.93
v_{ram}	-0.23	0.01	0.20	0.17	0.81
v_{cap}	-0.59	0.04	-0.02	1.28	0.85
d_{cap}	-0.23	0.01	-0.53	2.06	0.75
e_{ram_f}	-23.92	1.04	17.61	3.71	0.87
τ_{final}	-6.03	-0.11	-0.25	11.60	0.66
c_{fp}	0.35	0.00	0.07	0.19	0.85
d_{pmax}	-0.23	0.00	-0.48	2.11	0.82

• The hammer cushion only goes into tension; in this case Equation 13 is transformed to

$$K = \begin{bmatrix} 0 & 0 & 0 \\ 0 & k' & -k' \\ 0 & -k' & k' \end{bmatrix} \quad (34)$$

• Both cushions are in tension; the matrix of Equation 13 is null. The effects of these will be more clearly illustrated with the case studies.

The results of the parametric study can be seen in Table 2, the values for the acceleration, velocity and displacement y values being peak values of those parameters. The concept of the pile force coefficient c_{fp} is explained in Warrington (2020).

These variables can be ordered to more clearly compare them; however, there are two variables which will be taken out of the ordering because their slopes tend to be much larger than the others and obscure those results. The first is τ_{final} , which is interesting from an analytical standpoint (and also estimates the actual duration of the impact) but is probably the least important parameter under consideration. The largest absolute slope value for this parameter is $m_{k'}$, and this shows that the time of analysis increases with decreasing k' , or softer pile cushions.

The other variable that should be considered separately is e_{ram_f} , the ratio of the rebound energy to the impact energy. This is a significant parameter and the best way to illustrate its variance is by looking at specific cases. The variation of e_{ram_f} with m' and z' for $k' = 0.1, 0.5$ and 1.0 is shown in Figures 11, 12, and 13 respectively.

The slope variables indicate that e_{ram_f} increases with decreasing k' and has the opposite effect with decreasing z' , and Figures 11, 12, and 13 bear this out. The values of e_{ram_f} tend to be considerably higher than those for steel piles, especially with softer pile cushions. This is potentially significant and deserves further study.

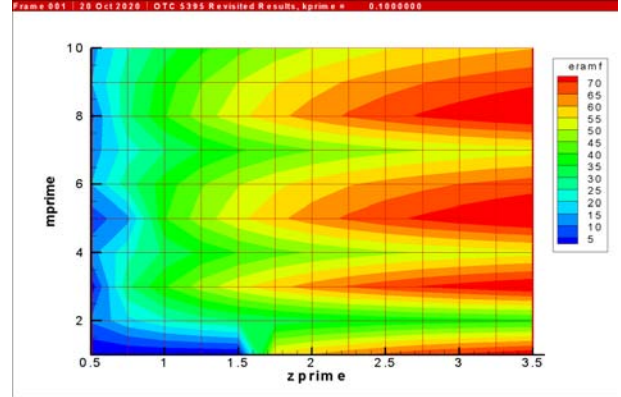


Figure 11. Parametric Study of e_{ram_f} for Ranges of z' and m' , $k' = 0.1$

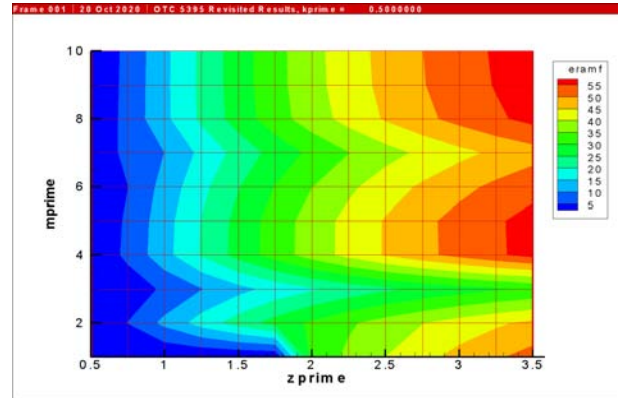


Figure 12. Parametric Study of e_{ram_f} for Ranges of z' and m' , $k' = 0.5$

Turning to the other variables, the coefficient of determination and the three slopes are re-ordered and shown in Figures 14, 15, 16 and 17.

From these figures the following can be seen:

1. The coefficient of determination varies from parameter to parameter, the highest being a_{cap} and the lowest being a_{ram} (Figure 14.) A low R^2 only means that the modelling of a particular parameter is not truly linear.
2. For $m_{k'}$, the variable that varies the most with changes in k' is v_{cap} , which increases with a softening pile cushion (Figure 15,) as is the case with e_{ram_f} . The slope for a_{cap} is also negative but slightly less than that for v_{cap} . On the other side is the slope for c_{fp} , which increases with a hardening pile cushion. This also makes sense because the motivation behind increasing the pile cushion thickness is to decrease the pile head forces and stresses.
3. For $m_{m'}$, the highest slope (both in terms of absolute value and otherwise) is that for a_{cap} , which means that cap acceleration is decreased by increasing the mass of the cap.
4. For $m_{z'}$, the highest slopes are both negative and include both the cap and pile head displacements d_{cap} and d_{pmax} . As

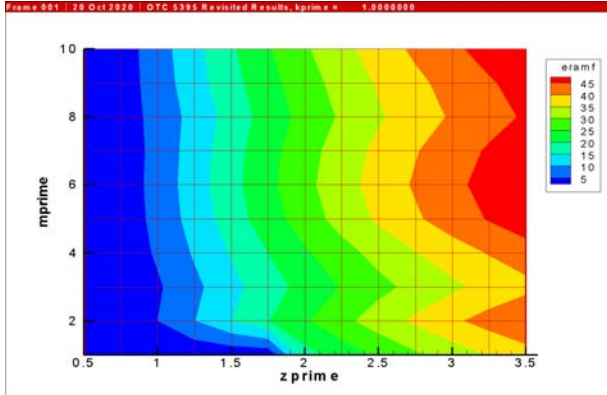


Figure 13. Parametric Study of e_{ram_f} for Ranges of z' and m' , $k' = 1.0$

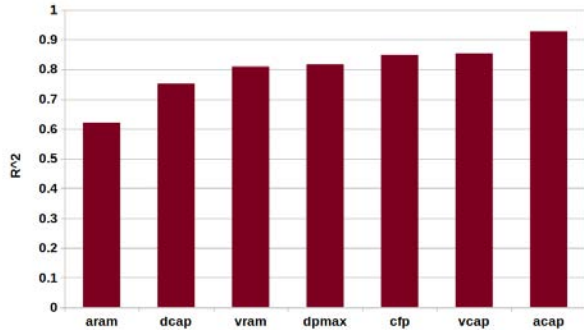


Figure 14. Coefficients of Determination for Parametric Study

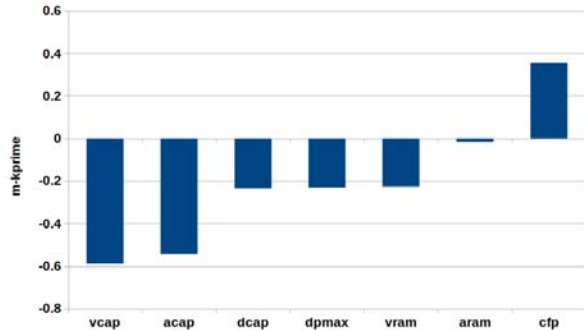


Figure 15. m_k for Parametric Study

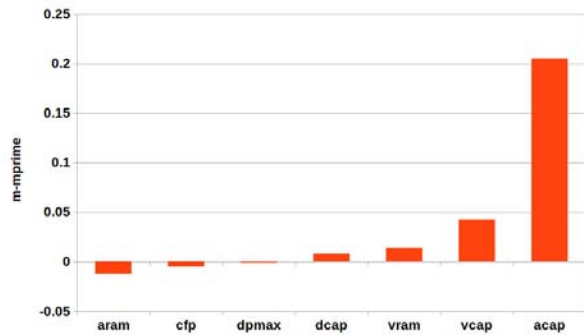


Figure 16. $m_{m'}$ for Parametric Study

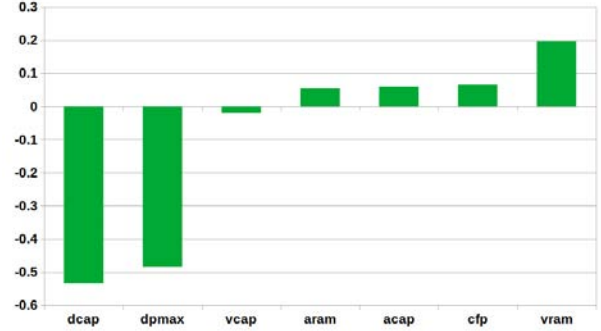


Figure 17. m_z for Parametric Study

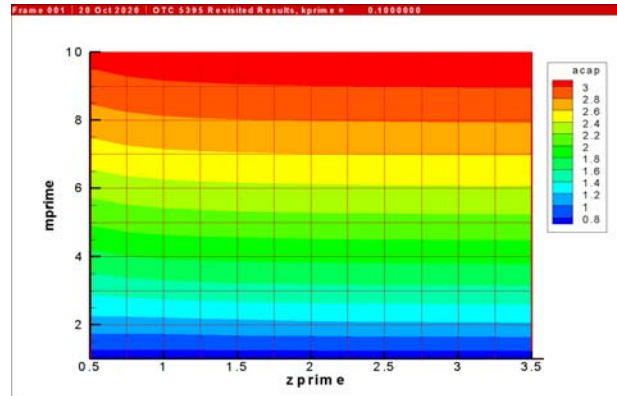


Figure 18. Variation of a_{cap} with z' and m' for $k' = 0.1$

is the case with steel pile, lower impedance piles move more with impact than higher impedance ones.

Some additional information can be obtained by a selection of parametric plots. The variation of a_{cap} with m' and z' for $k' = 0.1, 0.5$ and 1.0 is shown in Figures 18, 19 and 20 respectively. It is clear that the main independent variable that determines the value of a_{cap} is m' , as indicated in Figure 16. It is also clear that, as k' increases, a_{cap} decreases, as indicated in Figure 15.

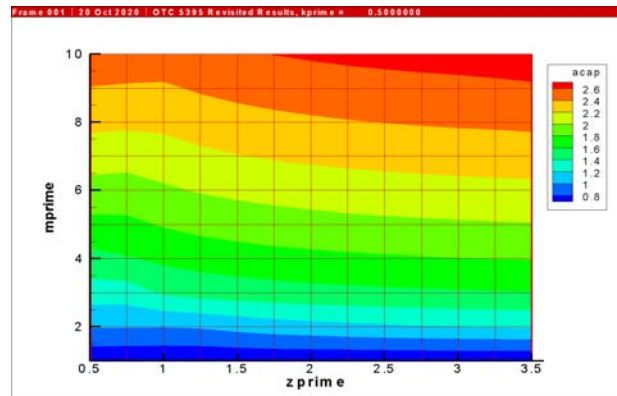


Figure 19. Variation of a_{cap} with z' and m' for $k' = 0.5$

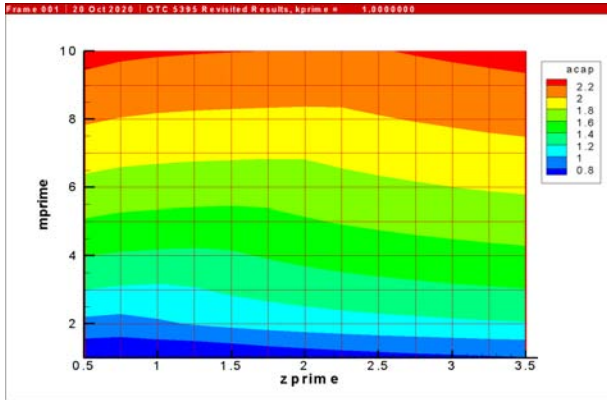


Figure 20. Variation of a_{cap} with z' and m' for $k' = 1.0$

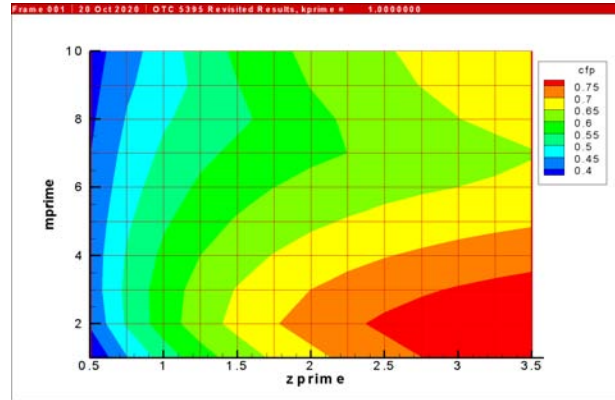


Figure 23. Variation of c_{fp} with z' and m' for $k' = 1.0$

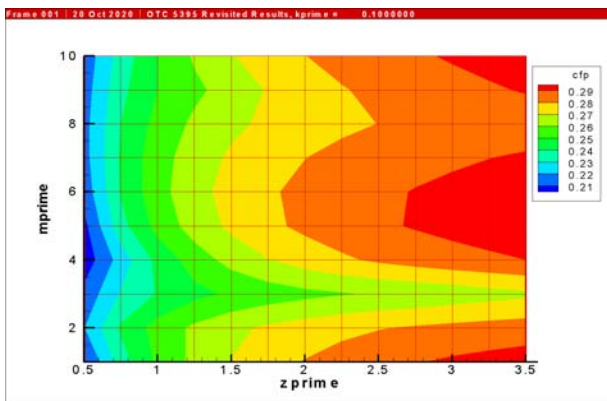


Figure 21. Variation of c_{fp} with z' and m' for $k' = 0.1$

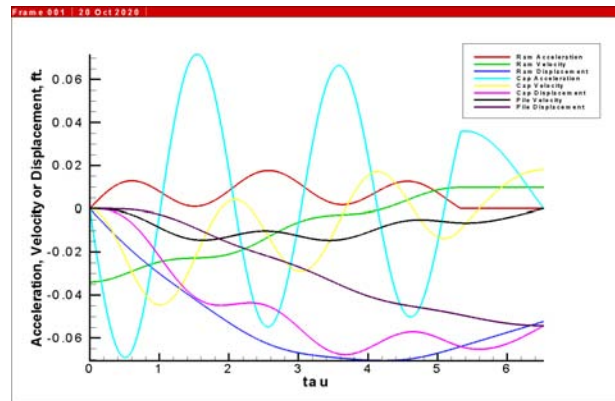


Figure 24. Numerical Solution, 12" Concrete Pile, Vulcan 06 with 6" Cushion

Figures 21, 22 and 23 are a similar presentation for the pile force coefficient c_{fp} . Although the general trend is for this to be more independent of m' and more dependent upon z' , there are many exceptions, and generalisations of this kind are not well supported by the data. The variation of c_{fp} is more significant for higher values of k' (stiffer pile cushions) than with lower ones.

Case Studies

Vulcan 06. This case study is the same as was done for the rigid pile head. As was the case there, there are two cases considered: a 6" pile cushion and an 18" pile cushion. The time history is shown in Figures 24 and 25. In both cases it is possible to see the two-frequency regime shown in Figures 2 and 3. What is different, however, is the effect on the inextensibility on the impact sequence. With the 6" cushion, the ram remains in contact with the cap until it disengages towards the end of the cycle, although the oscillation due to the higher frequency can be seen. With the 18" cushion the ram actually impacts the cap through its cushion four separate times, and the cap response is likewise more irregular than before. This type of "chatter" was seen with low impedance piles in Warrington (2020).

Table 3 shows the results not presented earlier in tabular form. The cap acceleration increases slightly with the softer pile cushion, as does the ram acceleration. The ram force coefficient (see Warrington (2020)) increases slightly with the softer pile cushion but the pile force coefficient (and with it the maximum pile stress) decrease, as one would expect. The energy returned to the ram increases dramatically with

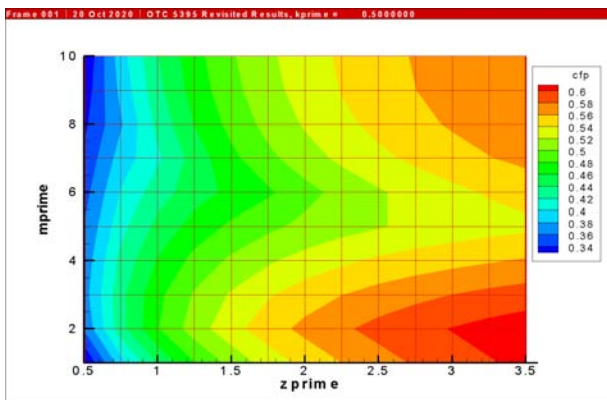


Figure 22. Variation of c_{fp} with z' and m' for $k' = 0.5$

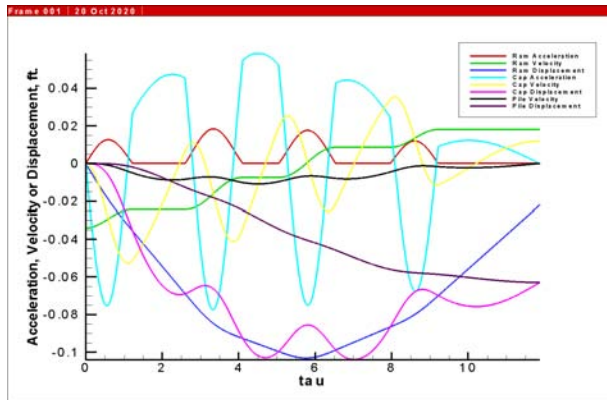


Figure 25. Numerical Solutions, 12" Concrete Pile, Vulcan 06 with 18" Cushion

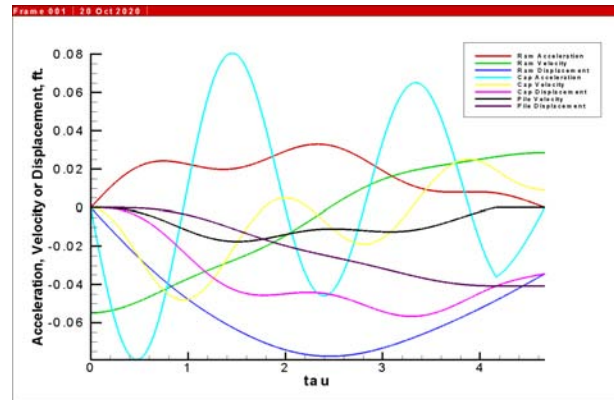


Figure 26. Numerical Solutions, 36" Concrete Pile, Vulcan 530 with 6" Cushion and Light Cap

Table 3

Results for Vulcan 06 Test Case

Parameter	6" Pile Cushion	18" Pile Cushion
z'	0.8581144	0.8581144
m'	6.310679	6.310679
k'	0.3828769	0.1276256
p_1	0.5050700	0.3169850
p_2	3.077629	2.831184
p_{rat}	6.093469	8.931603
k_{cush} , kips/ft	8640.000	2880.000
a_{ram_g} , g	61.02334	63.87626
a_{cap_g} , g	249.3005	268.6106
v_{ram_f} , ft/sec	3.262095	6.041542
$v_{p_{max}}$, ft/sec	4.907065	3.624857
$f_{p_{max}}$, lbs.	284314.6	210023.6
$\sigma_{p_{max}}$, psi	1974.407	1458.497
e_{ram_f}	8.227419	28.22058
c_{f_s}	0.5165500	0.5406994
c_{f_p}	0.3702560	0.2735087

the softer pile cushion.

Vulcan 530. In addition to the two different cushion thicknesses of the previous case, two different cap weights will be considered, making the total number of case options four. The light cap weighs 6,200 lbs. and the heavy cap weighs 16,000 lbs. The time plots of the results are shown in Figures 26, 27, 28 and 29.

The tabular data is shown in Table 4. From both the figures and the table, the following can be observed:

- Combining the 18" cushion with the heavy cap resulted in the same kind of ram and cap chatter that was seen in Figure 25.
- The ram acceleration and ram force coefficient is little affected by the changes in cap weight and pile cushion stiffness.
- With the light cap, the lower cushion stiffness led to a

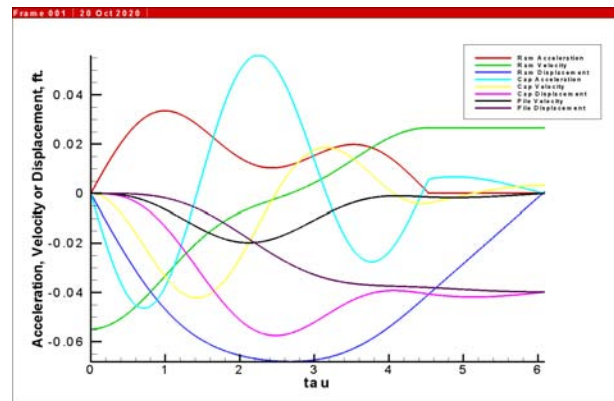


Figure 27. Numerical Solutions, 36" Concrete Pile, Vulcan 530 with 6" Cushion and Heavy Cap

much higher peak acceleration of the cap. With the heavy cap, there was little difference between the two.

- The 18" pile cushion significantly decreased the pile head forces and stresses, as would be expected. The pile head stresses tended to be higher for the heavy cap than the light one.
- The heavy caps tended to reduce the energy returned to the ram in rebound. Whether this increases the peak force and stress on the pile is an open question.

Special Topics

The data analysed, there are some important topics that need to be considered.

System Length and Pile Head Stresses

Although the variation in pile head force and stress with variations of k' , m' and z' is well described above, the single most important variable is the system length. As evident in Equations 27 and 28, all other things being equal the peak results of the equations are linearly proportional to the sys-

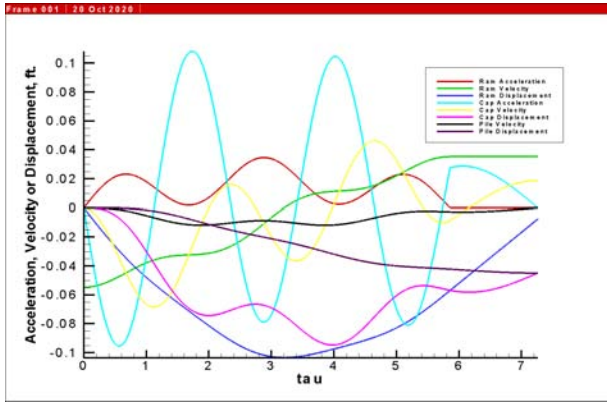


Figure 28. Numerical Solutions, 36'' Concrete Pile, Vulcan 530 with 18'' Cushion and Light Cap

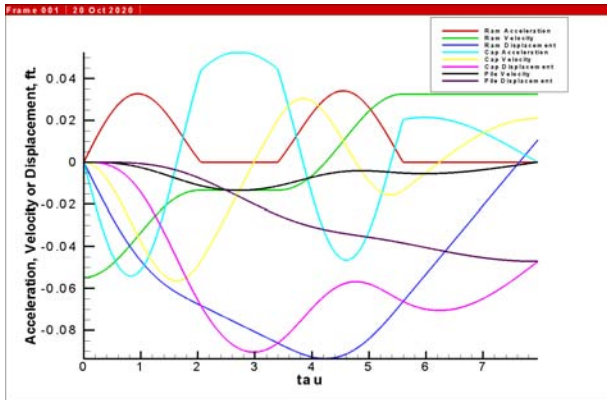


Figure 29. Numerical Solutions, 36'' Concrete Pile, Vulcan 530 with 18'' Cushion and Heavy Cap

Table 4
Results for Vulcan 530 Test Case

Parameter	6'' Pile Cushion Light Cap	18'' Pile Cushion Light Cap	6'' Pile Cushion Heavy Cap	18'' Pile Cushion Heavy Cap
z'	2.089437	2.089437	2.089437	2.089437
m'	4.838710	4.838710	1.875000	1.875000
k'	1.164107	0.3880356	1.164107	0.3880356
p_1	0.7169800	0.5015247	0.6902472	0.4634225
p_2	3.310200	2.732174	2.140388	1.840599
p_{rat}	4.616865	5.447736	3.100900	3.971753
k_{cush} , kips/ft	66,798.00	66,798.00	66,798.00	66,798.00
a_{ramg} , g	73.44598	77.00083	74.54994	75.87357
a_{capg} , g	179.4863	241.2977	124.9715	120.5316
v_{ramf} , ft/sec	7.631509	9.427312	7.116651	8.717998
v_{pmax} , ft/sec	4.723139	3.174867	5.316308	3.598206
f_{pmax} , lbs.	2,462,921.	1,655,562.	2,772,234.	1,876,315.
σ_{pmax} , psi	1900.402	1277.439	2139.070	1447.774
e_{ramf}	27.01732	41.22847	23.49485	35.25778
c_{fs}	0.6013253	0.6304300	0.6103638	0.6212007
c_{fp}	0.6721570	0.4518201	0.7565718	0.5120661

tem length. Some discussion of this important input parameter is in order.

To begin the discussion, substituting Equation 2 into Equation 15 yields

$$L_{sys} = \frac{V_0}{\sqrt{\frac{k_1}{m_1}}} \quad (35)$$

Since, for single acting hammers (or using an effective stroke)

$$V_0 = \sqrt{2ges} \quad (36)$$

the system length can be shown to be

$$L_{sys} = \sqrt{\frac{2gesm_1}{k_1}} \quad (37)$$

Since

$$E_n = W_1 es = gm_1 es \quad (38)$$

the system length can be expressed as

$$L_{sys} = \sqrt{\frac{2E_n}{k_1}} \quad (39)$$

In simple terms, there are two ways of increasing the system length: increasing the net striking energy or decreasing the stiffness of the hammer cushion. This result is independent of how the energy is obtained, i.e., whether the stroke is long and the ram light or the stroke short and the ram heavy. This has been a long-running issue with impact pile hammers (Hirsch and Samson (1966); Rausche, Likins, Miyasaka, and Bullock (2008).)

The cushion configuration of many hammers (physical, material and/or both) is considered a “given” with the hammer and is frequently represented in this way (Goble and Rausche (1986).) But this is not necessarily the case. With hammers that use a “full” anvil, such as diesel hammers or the single-compound hammer (Mondello and Killingsworth (2014); Warrington (2016),) the cushion is almost independent of the hammer because the hammer places few physical constraints on its size. With air/steam hammers, there have been many changes over the years. Those that used cushion generally started out using wood for cushion. Raymond Concrete Pile Company introduced the capblock shield (Vulcan referred to this as the capblock follower) which used stiffer micarta and aluminium cushion but in a taller cushion stack. Other manufacturers are very specific about the type of material to be used and its configuration.

Based on Equation 39, it would seem that softening the hammer cushion would, by increasing the system length, increase all of the parameters at the pile head. This seems counter-intuitive, and an example will show that the suspicion is justified.

Table 5
Results for Vulcan 530 Test Case with Softened Hammer Cushion

Parameter	6" Pile Cushion Light Cap	18" Pile Cushion Light Cap	6" Pile Cushion Heavy Cap	18" Pile Cushion Heavy Cap
z'	2.089437	2.089437	2.089437	2.089437
m'	4.838710	4.838710	1.875000	1.875000
k'	2.328213	0.7760711	2.328213	0.7760711
p_1	0.8283519	0.6394030	0.8147240	0.6059574
p_2	4.051925	3.030686	2.564493	1.990716
p_{rat}	4.891550	4.739868	3.147683	3.285240
k_{cush} , kips/ft	33,399.00	33,399.00	33,399.00	33,399.00
a_{ramg} , g	59.25720	57.14347	54.88093	52.11800
a_{capg} , g	103.2307	153.9869	65.07989	103.9744
v_{ramf} , ft/sec	8.830050	9.858164	8.097713	9.497916
v_{pmax} , ft/sec	3.782344	3.160125	4.477098	3.597403
f_{pmax} , lbs.	1,972,336.	1,647,874.	2,334,621.	1,875,896.
σ_{pmax} , psi	1521.864	1271.508	1801.405	1447.451
e_{ramf}	36.16995	45.08307	30.41908	41.84833
c_{fs}	0.6861161	0.6616421	0.6354450	0.6034541
c_{fp}	0.7612302	0.6360032	0.9010555	0.7240092

In this example, the Vulcan 530 test case is reconsidered by cutting the cushion stiffness in half to 33,399 kips/ft, which increases the system length by a factor of $\sqrt{2}$ to 0.078 ft. (Compare these with the original parameters in Table 1.) The results were rerun with this change and they are summarized in Table 5.

Comparison of Tables 4 and 5 shows the following:

- Both the ram and cap peak decelerations decrease significantly with the softer hammer cushion.
- For the 6" pile cushion cases, both the peak pile head forces and stresses decrease with the softer hammer cushion. Although this may be useful if stress control is the primary issue, decreasing the pile head force decreases the force the pile in turn exerts on the soil and advances into the ground, which adversely affects the drivability of the pile. The difference with the 18" pile cushion is much smaller.

• The rebound energy back into the ram increases with the softer hammer cushion. This indicates a less efficient energy transfer mechanism, even without hysteresis effects or movement of the entire pile taken into consideration. This result illustrates the weakness of over-reliance on the system length as the key parameter for pile head response. All of the parametric studies in this and Warrington (2020) assume a constant system length, which assumes either a) a fixed hammer-hammer cushion configuration or b) a series of hammers with a fixed system length, which is unlikely. The parametric studies are interesting but caution must be exercised in making generalizations from them.

Returning to the issue of ram weight/stroke relationship, no generalization about this can be made without some con-

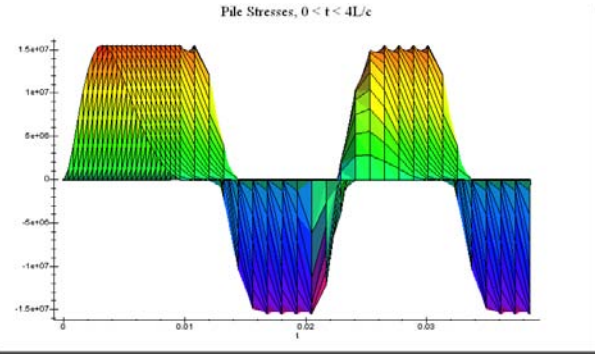


Figure 30. Illustration of Pile Stresses in a Bar Free on Both Ends

sideration of the hammer cushion configuration, which is a crucial part of the force-time characteristics of the system. It should also be observed that this model does not consider either geotechnical interactions with the soil or cushion instability due to elevated stresses and high impact velocities. If a hammer configuration is “set” for a given driving scenario, then Equation 35 indicates that the only parameter that can be changed to induce changes in the pile head response is the impact velocity, which in turn leads to consideration of the stresses which result from impact. If pile stresses are an important consideration—and this is frequently the case with concrete piles—then limiting this velocity is an important component in controlling pile stresses.

Tensile and Compressive Stresses

The methods described here predict the magnitude and time history of the pile head displacement, velocity, force and stresses. As has been the case since Isaacs (1931), the core problem with concrete piles during driving is overstressing them in tension. The stresses shown in this study are compressive stresses. So how can this be used to control these important tension stresses?

The simplest way to get to an answer to this is to consider the fact that, when a bar is struck on one end and a compressive stress wave is produced, if the bar is free on the other end, a tension stress wave of the same magnitude is reflected, assuming that the bar is long enough so that the two processes (wave generation on one end, reflection on another) are independent of one another. (Some discussion of what happens when the two waves overlap is given in Timoshenko and Goodier (1951).) This is illustrated in Figure 30. The pile is being viewed from “on end,” with time from initial impact at the abscissa and pile stresses on the ordinate. The initial impact is shown by the positive wave on the far left; the negative wave to its right is the reflection from the free toe. The subsequent reflections are of opposite direction because, after the initial impact, the bar is modelled as having two free ends (Warrington (1997).)

A concrete pile in the early stages of driving, lacking substantial shaft and toe resistance, is about as close to a free-ended undamped bar as is encountered with driven piles. That being the case, it is evident that the compressive stress is an upper bound to the possible tensile stress in rebound. To control the stress with the hammer-pile system in place, it is necessary to control the system length. Equation 39 indicates that, for a given k_1 , the system length varies with the square root of the net striking energy (or the rated energy if the efficiency is constant.)

For example, with the Vulcan 530 using a 6" pile cushion and the original hammer cushion, the compressive stress at full energy is 2,139 psi. To obtain a stress of 700 psi, the energy would have to be reduced to approximately 11% of rated striking energy. Usually such a drastic reduction is not necessary due to the fact that some resistance is encountered even in the early stages of driving, although in some cases a smaller hammer is used to initiate driving. Nevertheless it illustrates that controlling the impact velocity in the early stages of driving is crucial for successful concrete pile driving.

Effect of Oscillations on Pile Cushion Energy Transmission

As was the case with Warrington (1987) and Warrington (2020), the model presented here does not include the effects of losses due to hysteresis in the hammer or pile cushion. These losses are important but, as is evident from Warrington (1997), inclusion of same considerably complicates the mathematics of the solution. Although much of this complication can be avoided using a numerical method, this still adds another independent variable to consider.

Although the most common method in vibration to account for these types of losses is viscous (velocity-dependent) damping, in impact pile driving the most common method used is to model a bilinear cushion as Smith (1960) did. In either case, repeated cycling of the cushion material will result in additional losses with actual cushion material, in addition to the losses predicted using the purely elastic model. If viscous damping is used, this tends to act as a "high-pass filter" for applications such as this, and higher frequencies are an inevitable result of the two degree-of-freedom system that constitutes a hammer-cap system atop a concrete pile with both hammer and pile cushion.

Combined with the elevated rebound energies predicted by the model, it is difficult to avoid the conclusion that, as currently practised, methods used to set up hammer-cap-cushion systems for concrete piles are not efficient in their energy transmission.

Conclusions

1. The addition of a pile cushion to the hammer-cap-cushion system adds considerable complexity to the response

of the system to impact, along with another independent variable (k') to consider.

2. A bi-harmonic condition exists for this type of vibrating system, which leads to the existence of vibrating frequencies which are both lower and higher than the fundamental frequency ω_0 of the hammer-hammer cushion system. There is the possibility of greater energy losses in the pile cushion due to higher frequency vibrations.

3. The impedance ratio of the piles is greater than those encountered in steel piles. However, the cap accelerations and velocities tend to be greater due to the softness of the pile cushion.

4. The simplest way to attenuate higher cap accelerations—and to stabilize the impact—is to increase the weight/mass of the cap relative to that of the ram.

5. Increasing the pile cushion thickness (and decreasing its stiffness) is effective in reducing pile stresses, but there are other effects (rebound energy, stability of impact) to consider. Reducing the system length via the impact velocity, either during part or all of driving, is an important way to control stresses due to impact.

6. System length is directly proportional to the square root of the striking energy and inversely proportional to the square root of the hammer cushion stiffness. With a fixed energy, softening the hammer cushion would seem to be a method of increasing pile head velocity (and thus force,) but the changes in other parameters offsets this substantially.

7. The parametric studies are important but, because they assume a constant system length, their broad application must be done with caution.

8. The method can be used to control tensile stresses as well as compressive ones, as it sets an upper bound for those stresses.

Nomenclature

ω_0	Ram-cushion natural frequency, rad/sec
ω_1	Lower biharmonic frequency, rad/sec
ω_2	Upper biharmonic frequency, rad/sec
ρ	Density of pile material, $\frac{kg}{m^3}$ or $\frac{slugs}{ft^3}$
$\sigma_{p_{max}}$	Peak pile head stress, Pa or psf
τ	Dimensionless time, radians
τ_{final}	Stopping time of analysis
A_3	Pile cross-sectional area, m^2 or ft^2
a_{cap_g}	Peak cap acceleration g's
a_{cap}	Reduced cap acceleration, ft or m
a_{ram_g}	Peak ram acceleration g's

a_{ram}	Reduced ram acceleration, ft or m	t	Actual time, seconds
b	y-intercept of "plane"	v_0	Velocity vector
C	Damping matrix	v_{cap}	Reduced cap velocity, ft or m
c_{fs}	Ram force coefficient	v_{pmax}	Peak pile head velocity, m/sec or ft/sec
c_{fp}	Pile force coefficient	v_{ramf}	Final ram velocity, m/sec or ft/sec
d_{cap}	Reduced cap displacement, ft or m	v_{ram}	Reduced ram velocity, ft or m
d_{pmax}	Maximum pile head displacement, m or ft	W_1	Ram weight, N or lbs
E	Pile modulus of elasticity, Pa or psf	$X_n(\tau)$	Reduced displacement of ram (subscript $n = 1$) or cap (subscript $n = 2$), m or ft
e	Mechanical efficiency of hammer	z'	Impedance Ratio
E_n	Net striking energy, N or ft-lbs	Z_1	Hammer impedance, N-sec/m or lb-sec/ft
e_{ramf}	Proportion of ram energy returned to ram in rebound, percent	Z_3	Pile impedance, N-sec/m or lb-sec/ft
f_{pmax}	Peak pile head force, N or lbs.	y	Parameter resulting from "planar" regression
g	Acceleration due to gravity		
K	Stiffness matrix		
k'	Cushion Stiffness Ratio		
k_1	Hammer Cushion Stiffness, N/m or lb/ft		
k_2	Pile cushion stiffness, N/m or lb/ft		
k_{cush}	Hammer cushion stiffness, N/m or lb/ft		
L_{sys}	System length, m or ft		
M	Mass matrix		
m'	Cap-Ram mass or weight ratio		
m_1	Ram mass, kg or slugs		
m_2	Cap mass, kg or slugs		
$m_{k'}$	Slope of "plane" due to k'		
$m_{m'}$	Slope of "plane" due to m'		
$m_{z'}$	Slope of "plane" due to z'		
p_1	Lower frequency ratio to fundamental frequency		
p_2	Upper frequency ratio to fundamental frequency		
p_{rat}	Ratio of frequencies of biharmonic system		
s	Laplace transformed variable for τ		
s	Stroke or effective stroke of hammer, m or ft		

References

- Deeks, A. J., & Randolph, M. (1993, May). Analytical modelling of hammer impact for pile driving. *International Journal for Numerical and Analytical Methods in Geomechanics*, 17, 279–302. doi: 10.1002/nag.1610170502
- den Hertog, J. (1985). *Mechanical vibrations* (Fourth ed.). Dover Publications, Inc.
- Goble, G., & Rausche, F. (1986). *Weap86: Wave equation analysis of pile foundations*. Federal Highway Administration.
- Heerema, E. (1980, May). An evaluation of hydraulic vs. steam pile driving hammers. *Proceedings of the Twelfth Annual Offshore Technology Conference*, 321–330.
- Hirsch, T., & Samson, C. (1966). *Driving practices for prestressed concrete piles*. Texas Transportation Institute.
- Isaacs, D. (1931, September). Reinforced concrete pile formulae. *Journal of the Institution of Engineers Australia*, 3(9), 305–323.
- Kreyszig, E. (1988). *Advanced engineering mathematics* (Sixth ed.). John Wiley & Sons, Inc.
- Meirovitch, L. (2001). *Fundamentals of vibrations*. Wave-land Press.
- Mondello, B., & Killingsworth, S. (2014). *Dynamic pile testing results, Crescent Foundation demonstration test pile – Vulcan SC9 hammer, Kenner, Louisiana* (Tech. Rep.).
- Parola, J. F. (1970). *Mechanics of impact pile driving* (Unpublished doctoral dissertation). University of Illinois at Urbana-Champaign.

- Rausche, F., Likins, G., Miyasaka, T., & Bullock, P. (2008). The effect of ram mass on pile stresses and pile penetration. *Proceedings of the Eighth International Conference on the Application of Stress-Wave Theory to Piles*, 389–394.
- Smith, E. (1960). Pile driving analysis by the wave equation. *Journal of the Soil Mech. Found. Eng. Div., ASCE*, 86.
- Starkey, B. (1954). *Laplace transforms for electrical engineers*. Illiffe and Sons, Ltd.
- Take, W., Valsangkar, A., & Randolph, M. (1999, September). Analytical solution for pile hammer impact. *Computers and Geotechnics*, 25(2), 57–74. doi: 10.1016/S0266-352X(99)00018-X
- Thompson, W. T. (1965). *Vibration theory and application*. Prentice-Hall, Inc.
- Timoshenko, S., & Goodier, J. (1951). *Theory of elasticity* (Second ed.). McGraw-Hill Book Company, Inc.
- Timoshenko, S., & Young, D. (1955). *Vibration problems in engineering* (Third ed.). D. Van Nostrand Company, Inc.
- Warrington, D. C. (1987, April). A proposal for a simplified model for the determination of dynamic loads and stresses during pile driving. *Proceedings of the Offshore Technology Conference*, 329–338. doi: 10.4043/5395-MS
- Warrington, D. C. (1997). *Closed form solution of the wave equation for piles* (Unpublished master's thesis). University of Tennessee at Chattanooga, Chattanooga, TN.
- Warrington, D. C. (2016). *Improved methods for forward and inverse solution of the wave equation for piles* (Unpublished doctoral dissertation). University of Tennessee at Chattanooga, Chattanooga, TN.
- Warrington, D. C. (2020). *Otc 5395 revisited: Analysis of cushioned pile hammers* (Tech. Rep.). doi: 10.13140/RG.2.2.10487.04002/1